***Electrodialysis, especially reverse, is a promising method of water desalination, concentration of solutions, extraction of valuable components from waste and rinse water, and power generation. The main problem is the search for low-cost universal anode-cathode materials. The work aims to determine the possibility of using the VNZh90 superalloy (5 % Ni, 5 % Fe, 90 % W) and the electroplated Ni-W alloy as a universal cathode-anode material for reverse electrodialysis. The crystal structure of the Ni-W alloy was studied by X-ray diffraction analysis; the morphology was studied by scanning electron microscopy. The anodic behavior of both alloys was studied by voltammetry in 6 % HCl in a saturated NaCl solution.***

***The high passivity of the VNZh90 superalloy was revealed. On the repeated anodic curve, the current density of the passivation plateau decreased 2.8 times and was 37 mA/dm$^2$. This indicates that the use of the VNZh90 superalloy is promising as a universal cathode-anode material of a reverse electrodialyzer.***

***The phenomenon of significant passivation for the Ni-W alloy was also revealed. The primary curve of the alloy showed two dissolution peaks and a well-defined passivation plateau. Probably, the first peak corresponded to a more active phase with a low W content. This was confirmed by the absence of the first peak on the repeated anodic curve and the identity of the passivation plateaus of the primary and repeated curves. The passivation current density was 209 mA/dm$^2$. These data also indicate the possibility and prospects of using the electroplated Ni-W alloy as a universal cathode-anode material of a reverse electrodialyzer after optimizing the composition and deposition method of the alloy, as well as reducing the wear rate***

***Keywords: reverse electrodialysis, universal electrode, superalloy, passivation, anodic behavior, tungsten, nickel***

UDC 54.057:544.653:621.13:661.13
DOI: 10.15587/1729-4061.2021.239015

# DETERMINATION OF THE APPLICABILITY OF THE TUNGSTEN-CONTAINING MATERIAL AS LOW-COST ELECTRODES FOR REVERSE ELECTRODIALYSIS

**Vadym Kovalenko**
*Corresponding author*
PhD, Associate Professor
Department of Analytical Chemistry and
Chemical Technology of Food Additives and Cosmetics*
Senior Researcher**
E-mail: vadimchem@gmail.com
**Valerii Kotok**
PhD, Associate Professor
Department of Processes, Apparatus
and General Chemical Technology*
Senior Researcher**
*Ukrainian State University of Chemical Technology
Gagarina ave., 8, Dnipro, Ukraine, 49005
**Competence center
"Ecological technologies and systems"
Vyatka State University
Moskovskaya str., 36, Kirov,
Russian Federation, 610000

*Received date 28.06.2021*
*Accepted date 12.08.2021*
*Published date 26.08.2021*

***How to Cite:*** *Kovalenko, V., Kotok, V. (2021). Determination of the applicability of the tungsten-containing material as low-cost electrodes for reverse electrodialysis. Eastern-European Journal of Enterprise Technologies, 4 (12 (112)), 39–46. doi: https://doi.org/10.15587/1729-4061.2021.239015*

## 1. Introduction

The Sustainable Development Strategy is an effective direction for the development of civilization. Sustainable development is based on the following basic principles:

a) recycling or reuse of materials;

b) maximum use of clean energy or energy derived from renewable sources;

c) prevention of environmental pollution.

Electricity and drinking water are among the most problematic resources [1]. In many countries, drinking water is obtained from excessively saline or sea water by the method of electrodialysis [2]. However, in the presence of two and polyvalent metal cations in water, precipitation is formed during electrodialysis, both on membranes and in electrode spaces. To prevent this process, as well as to conduct electrodialysis of concentrated solutions, reverse electrodialysis is used [3, 4]. This method is promising and widely used for various purposes. With the help of reverse electrodialysis, it is possible to obtain drinking water [2], concentrate sulfuric acid [5], and reduce the content of anionic dyes, for example, Acid Orange 7 [6]. At the same time, reverse electrodialysis can be used to generate electric power during heat recovery in the form of a heat engine [7, 8], using artificial solutions (for example, ammonium bicarbonate [9]) or microorganisms [10]. The method of power generation by reverse electrodialysis using a salinity gradient is even more efficient [11, 12]. In this case, a mixture of sea and river water [13], seawater or brines [14], as well as sea, river water, and/or artificial brines [15] can be used. The use of combined water treatment and power generation systems is effective [16]. Power generation using solutions of monovalent [17] and polyvalent [18] ions has been studied under laboratory conditions. The works [19, 20] show the possibility of scaling the method of power generation by reverse electrodialysis.

Reverse electrodialysis can be used to extract valuable components from wastewater, for example, $Ni^{2+}$ from galvanic wastewater [21].

In addition, electrodialysis can be used for the targeted production of metal hydroxides. In [22, 23], electrodialysis was used to obtain electrochemically highly reactive $Ni(OH)_2$. The authors showed that the use of electrodialysis production of nickel hydroxides is promising compared to other chemical (decomposition [24], two-stage high-temperature synthesis [25], homogeneous template deposition [26, 27], deposition at high [28, 29], and low [30, 31] supersaturation) and electrochemical methods (synthesis in a slot diaphragm electrolyzer [32, 33], including using a template [34]). It may be promising to replace the chemical synthesis of layered double hydroxides (LDH) (for example, Ni-Al LDH [35] and Zn-Al LDH [36, 37]) with the electrochemical synthesis in an electrodialyzer.

Although the promising method of reverse electrodialysis has many advantages and is widely used in technology, it has some disadvantages. In particular, the possibility of reproduction of microorganisms on ion-exchange membranes [38]. However, the most significant disadvantage is the problem of electrode materials. In reverse electrodialysis, the processes occurring on the electrodes change periodically. In this case, the anodes (oxidation processes occur) become cathodes (reduction processes occur) and vice versa. It should be noted that in the anodic mode, the electrodes must be insoluble. Few materials are known to operate in both the cathodic and anodic modes without the participation of electrode materials in the reaction. These are mainly precious metals of the platinum group. Therefore, the identification of low-cost materials that can work as a universal electrode (both anode and cathode) in a reverse electrodialyzer is very promising.

## 2. Literature review and problem statement

The problem of electrode materials for reverse electrodialysis is quite acute. Most of the publications generally ignore the issue of electrodes, focusing on ion-exchange membranes [11, 17]. The electrode materials described in the literature can be basically divided into two groups. The first group consists of mixed oxide electrodes. In [39], titanium electrodes coated with mixed Ru-Ir oxides were used. This electrode was used in dilute and saturated chloride solutions, similar to the ORTA electrode for electrolysis for the production of chlorine and alkali. However, it is known that ORTA electrodes are used only as anodes. In the cathodic mode, the oxides of ruthenium and titanium are reduced to metals, and after that, this electrode is no longer suitable for operation as an anode. Accordingly, during cathodic polarization on all electrodes, which are mixed oxide coatings on a titanium base, the oxides will be reduced to free metals both directly and by liberated ad-hydrogen atoms. As a result, during anodic polarization, the titanium base of the electrode will be passivated, and the electrode performance will sharply decrease. Therefore, mixed oxide electrodes can be used in reverse electrodialysis only if the anode period is short. The second group is metal electrodes based on platinoids. In [40], the authors used electrodes in the form of a niobium grid coated with Pt. These electrodes are absolutely inert and can effectively work both as a cathode and as an anode. However, these electrodes are very expensive, which significantly reduces the possibility of using large-size reverse electrodialysis units.

It should be noted that the search for low-cost universal electrode materials should be carried out precisely among metal electrodes. It is well known that any metal electrodes can effectively work as cathodes. However, in the case of monometallic electrodes, only noble metals exhibit the properties of an insoluble anode in any (acidic and alkaline) media, especially in the presence of strong depassivators. However, it is promising to study the anodic behavior of binary metal systems, in which one component is insoluble in an acidic medium and the other in an alkaline one. The most promising is the Ni-W system: Ni is strongly passivated in neutral and alkaline media, and W is passivated in acidic ones. Since the melting points of Ni and W are very different, this metal system can be obtained in two ways:

1) formation of a Ni-W superalloy by powder metallurgy;

2) electrochemical production of Ni-W alloy.

Superalloys are not true alloys but are a composite material (similar to organic-organic [41] and inorganic-inorganic composites [42]), consisting of particles of a solid component (W or WC) and particles of a binder metal (most often Ni or Co) [43, 44]. When pressed with heating, the binder metal is partially melted, connecting the particles of the solid component. In [45, 46], a method was developed for processing various superalloys by selective dissolution of the binder metal in an acidic electrolyte, followed by regeneration of the binder metal powder [47, 48]. It was shown that WC-based superalloys are easily processed. At the same time, a very high passivity of the VNZh90 superalloy (90 % W, 5 % Ni, 5 % Fe) was revealed. The high passivity of this alloy was confirmed during anodic oxidation in alkaline-ammonium solutions [49, 50] both at constant [51] and alternating current [52]. However, to confirm the possibility of using the VNZh90 alloy as a universal anode-cathode material of a reverse electrodialyzer, it is necessary to additionally study the anodic behavior of this alloy in the corresponding solutions.

Another promising material for a universal electrode is electroplated Ni-W alloy [53, 54]. Depending on the electrolyte and deposition conditions, coatings of various structures are formed [55], including nanocrystalline [56, 57] and amorphous [58] deposits. Ni-W coatings are used to form microdevices [59], and also as highly hard [60], magnetic (Ni-Fe-W) [61] and catalytically active [62] materials. In [63, 64], the authors studied the corrosion properties of the electroplated alloy and showed high corrosion resistance. However, to confirm the possibility of using the Ni-W alloy as a universal anode-cathode material of a reverse electrodialyzer, it is necessary to additionally study the anodic behavior of this alloy in the corresponding solutions.

## 3. The aim and objectives of the study

The study aims to determine the possibility of using the VNZh90 superalloy and the electroplated Ni-W alloy as a universal cathode-anode material for reverse electrodialysis.

To achieve the aim, the following objectives were set:

– to study the anodic behavior of the VNZh90 alloy in a solution corresponding to the electrolyte of the electrode space of the electrodialyzer;

– to study the characteristics and anodic behavior of the electroplated Ni-W alloy in a solution corresponding to the electrolyte of the electrode space of the electrodialyzer.

## 4. Research materials and methods

### 4. 1. Description of the sample of the investigated superalloy

The VNZh90 alloy of the following composition was used for the study: 90 % W (solid component), 5 % Ni, 5 % Fe (binder metal). The investigated sample of the VNZh90 alloy is the penetrator for armor-piercing munitions.

*The method of obtaining a coating with Ni-W alloy.*

Electrolyte composition and conditions for Ni-W coating (with W content 55–65 %) on Pt and Ni bases:

| | |
|---|---|
| $NiSO_4 \cdot 7H_2O$ | 90–100 g/l; |
| $Na_2WO_4.2H_2O$ | 200 g/l; |
| $(NH_4)_2SO_4$ | 37.5 g/l; |
| $C_4H_6O_6$ tartaric acid | 105 g/l; |

pH=3.5, $t$=75 °C, $i_k$=5 A/dm$^2$, coating time 40 minutes.

### 4. 2. Methods for studying the structure and morphology of electroplated Ni-W alloy

The crystal structure was studied by X-ray diffraction analysis (XRD) using a DRON-3 diffractometer (Russia) (Cu-Kα radiation, angle range 20–100° 2θ, scanning rate 0.1°/s). The morphology of the coating was studied using a 106-I scanning electron microscope (SEM) (SELMI, Ukraine).

### 4. 3. Method for studying anodic behavior

Anodic polarization characteristics were measured using a specially designed cell. As a working electrode, we used a VNZh90 superalloy sample (to supply current to the sample, a copper wire was wound and placed in specially prepared tubular PVC containers for isolation from the electrolyte) and a Ni-W alloy sample. Mesh platinum was used as a counter electrode. Reference electrode – Ag/AgCl (sat.). To assess the anodic behavior of W-containing materials, the most aggressive solution was chosen as the electrolyte, simulating the electrolyte of the anodic chamber of the electrodialyzer – a 6 % (wt.) HCl solution in a saturated NaCl solution. Polarization curves were recorded in a potentiodynamic mode using an Ellins P-8 potentiostat (Russia) with an anodic sweep from a stationary potential to a potential of +2,000 mV (for VNZh90 superalloy) and +1,000 mV (for electroplated Ni-W coating) with a sweep rate of 5 mV/s. Anodic polarization curves were recorded twice.

## 5. Results of studying the characteristics of W-containing materials

### 5. 1. Results of studying the anodic behavior of the VNZh90 alloy

Anodic polarization curves are shown in Fig. 1. On the primary anodic curve of the VNZh90 alloy, two dissolution peaks are observed, passing into the passivation plateau with a limiting current density of 100 A/dm$^2$.

The repeated curve shows a sharp decrease in both the currents of the dissolution peaks and the limiting current of the passivation plateau (up to 34 A/dm$^2$).

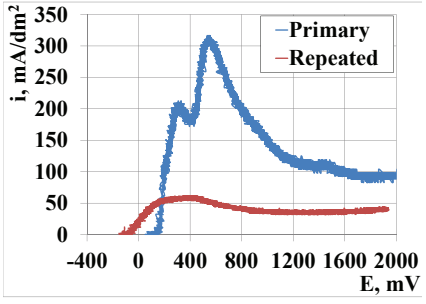


Fig. 1. Anodic polarization curves of the VNZh90 alloy

### 5. 2. Results of studying the characteristics and anodic behavior of the Ni-W alloy

The SEM images of the Ni-W coating surface (Fig. 2) show that the deposited coating is porous and has spherical inclusions in its structure, possibly just a nickel-tungsten alloy or metallic tungsten. Moreover, these particles have a submicron size or are nanoscale.

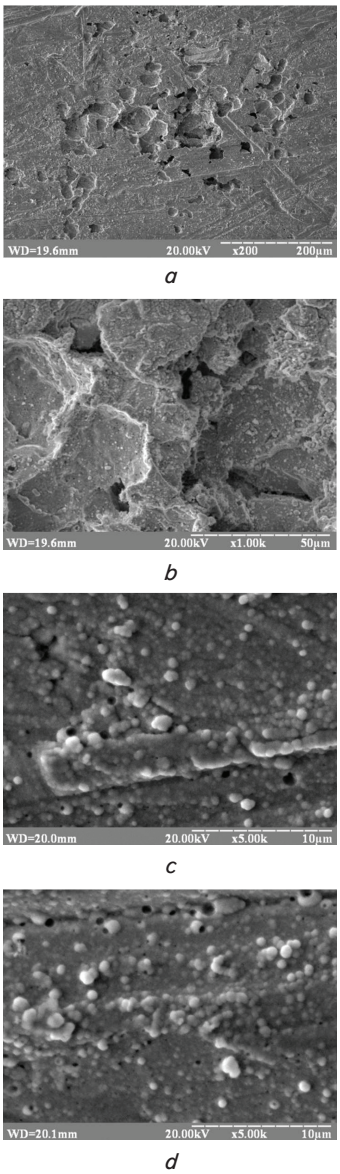


Fig. 2. SEM images of the Ni-W coating at different magnifications: *a* – ×200; *b* – ×1,000; *c*, *d* – ×5,000

For XRD, the Ni-W coating was applied to a steel base. Therefore, the diffractogram of the obtained alloy (Fig. 3) shows clear peaks of ferrite (the main component of the steel base). The diffractogram shows clearly pronounced peaks of the Ni-W alloy.

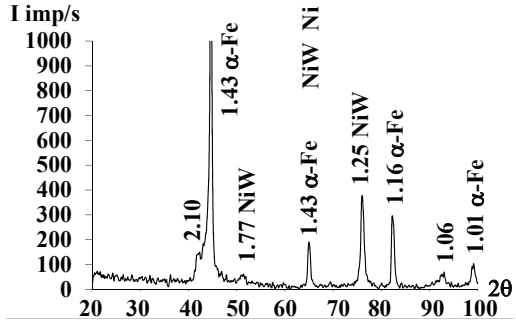


Fig. 3. X-ray diffractogram of the Ni-W coating

Anodic polarization curves of the Ni-W alloy are shown in Fig. 4. The results of the analysis of the digital characteristics of the polarization curves of the VNZh90 superalloy and the electroplated Ni-W alloy are given in Table 1.

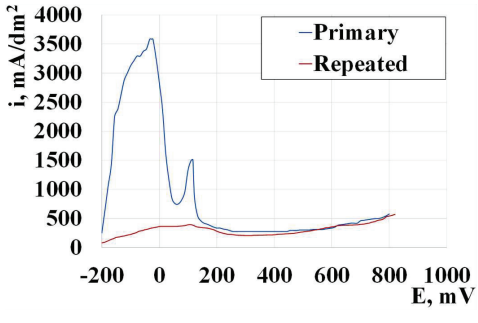


Fig. 4. Anodic polarization curves of the Ni-W coating

The primary polarization curve of the electroplated Ni-W alloy is in the form of the classic anode curve of the passivated metal. The curve shows two dissolution peaks, after which the formation of a passivation plateau with a limiting current of 270–280 mA/dm$^2$ is observed. The passivation plateau is observed starting from a potential of +180 mV. There are no sharp dissolution peaks on the repeated polarization curve; the passivation plateau, starting from a potential of +180 mV, practically coincides with the passivation plateau of the primary curve.

## 6. Discussion of the results of studying the characteristics of W-containing materials

The XRD data confirmed the deposition of the Ni–W alloy [53, 54]; no individual peaks of W were found on the diffractogram (Fig. 2). It should be noted that the resulting Ni-W alloy had a fairly high crystallinity. The data of scanning electron microscopy revealed the imperfection of the coating, the presence of pores in it (Fig. 3, *c, d*), and damage (Fig. 3, *a, b*). It should be concluded that it is necessary to optimize the deposition process. In addition, a prerequisite for using this coating as a universal anode-cathode material is its deposition to a strongly passivated substrate, in particular, titanium, zirconium, or niobium.

It was revealed that the polarization curves of the VNZh90 superalloy and the electroplated Ni-W alloy had a shape characteristic of the curve of passivated materials, corresponding to the literature data [45, 46].

It was found that for both alloys, the anodic polarization curves for the fresh surface of the alloy (primary curve) and the repeated polarization curves were fundamentally different (Fig. 1, 4).

For the VNZh90 alloy, the primary polarization curve (Fig. 1) had two anodic dissolution peaks, after which the dissolution current density sharply decreased, forming an indistinct passivation plateau with a constantly decreasing limiting current density. The first peak corresponded to the dissolution of Fe, the second peak – Ni. A sharp decrease in the dissolution current density allowed us to conclude that the alloy was significantly passivated. The repeated curves showed only one diffuse dissolution peak and a clearly defined passivation plateau. The dissolution peak potential on the repeated curve characterized the dissolution of Ni, while the dissolution peak of Fe was not observed. The current density of the Ni dissolution peak decreased from 306 mA/dm$^2$ (primary curve) to 59 mA/dm$^2$ (repeated curve), i.e. 5.18 times (Table 1). The limiting current density of the passivation plateau for the repeated polarization curve was 2.8 times lower than for the primary curve (Table 1). All these data indicate very significant passivation of the VNZh90 alloy. This can be explained by the fact that in a tungsten superalloy (which is VNZh90), W is able to dissolve in nickel, which leads to additional significant passivation of nickel even in the presence of strong depassivators. At the same time, tungsten is practically insoluble in Fe. When recording the primary polarization curve (Fig. 1), two peaks were observed and dissolution of nickel and iron occurred. As a result, the surface of the VNZh90 superalloy was depleted by the more active Fe-phase, and the proportion of the W solid component and passivated Ni increased. So, only the Ni dissolution peak was present on the repeated polarization curve (Fig. 1), the peak current densities and passivation plateaus were very significantly reduced. These data fully correlate with the data presented in [46] obtained in a slightly different electrolyte. Thus, the anodic behavior of the VNZh90 superalloy clearly indicates the possibility of using it as a universal cathode-anode material. The disadvantage of this material is that

Table 1

Electrochemical characteristics of anodic polarization curves of VNZh90 and Ni-W alloys

| Dissolution peak | | Passivation plateau | | Dissolution peak | | Passivation plateau | |
|---|---|---|---|---|---|---|---|
| *E*, mV | *i*, mA/dm$^2$ | *E*, mV | *i*, mA/dm$^2$ | *E*, mV | *i*, mA/dm$^2$ | *E*, mV | *i*, mA/dm$^2$ |
| VNZh90 alloy primary curve | | | | VNZh90 alloy repeated curve | | | |
| +295 | 193 | +1,190–+2,000 | 190–93 | +345 | 59 | +870–+1,880 | 37–39 |
| +525 | 306 | | | | | | |
| Electroplated Ni-W alloy primary curve | | | | Electroplated Ni-W alloy repeated curve | | | |
| –33 | 3,580 | +190–+690 | 275–380 | +100 | 390 | +190–+690 | 209–380 |
| +111 | 1,500 | | | | | | |

this alloy cannot undergo mechanical processing and must immediately be formed as a finished product. In addition, this alloy is still not cheap enough. However, the cost of the VNZh90 alloy can be reduced if it is made from recycled metal powders. Besides, when using this alloy as an anode, there is no need to impose high requirements for its mechanical characteristics. A possible direction of development can also be the manufacture and study of the anode characteristics of an alloy with a reduced tungsten content.

For the electroplated Ni-W alloy, the primary polarization curve (Fig. 4) also had two anodic dissolution peaks, after which a clearly pronounced passivation plateau was observed. The presence of two peaks probably indicates that the coating with the Ni-W alloy is likely to have a non-uniform distribution of the tungsten content over the depth and the upper thin layer, most likely, contains either pure Ni or Ni-W alloy with a minimum tungsten content. This component is much more active in the presence of a large number of chloride ions as strong depassivators and dissolves more actively. This is indicated by the 2.38 times higher current density of the first peak compared to the second one (Table 1). When the primary polarization curve is recorded, the active components dissolve and a passivation plateau is formed. This coating structure is confirmed by the repeated curve, in which the first dissolution peak of the active Ni-phase is absent, but the second peak, although weakly expressed, is present. And most importantly, the passivation plateaus of the primary and repeated curves are practically identical both in the potential interval and in the value of the limiting passivation current density. The data obtained also clearly indicate significant passivation of the electroplated Ni-W alloy and confirm the possibility of using this alloy as a universal cathode-anode material for reverse electrodialysis. However, it should be noted that the Ni-W alloy is characterized by significantly higher current densities compared to the VNZh90 superalloys: for the dissolution peak of 3,580 mA/dm$^2$ (Ni-W) and 306 mA/dm$^2$ (VNZh90), for the passivation plateau of 275 mA/dm$^2$ (Ni-W) and 93 mA/dm$^2$ (VNZh90) (Table 1). For the repeated polarization curve, the limiting current density of the electroplated Ni-W alloy is 209 mA/dm$^2$ compared to 37 mA/dm$^2$ (for the VNZh90 superalloy), i.e. 5.65 times higher (Table 1). That is, the service life of such an anode will be as many times lower. The advantage of an electroplated alloy is its significantly low cost, the possibility of applying it to substrates of any shape, and ease of production. The disadvantages include a high wear rate (dissolution). However, it should be noted that in this work, the alloy was deposited from only one electrolyte and in one production mode. There is reason to believe that in further studies, when optimizing the type of electrolyte and its composition, deposition parameters, and the W content in the alloy, the dissolution rate can be significantly reduced.

It should also be noted that the work has shown the possibility of using the VNZh90 superalloy and the electroplated Ni-W alloy as a universal cathode-anode material for a reverse electrodialyzer. However, for industrial use, it is necessary to carry out long-term (endurance) galvanostatic tests of these materials in the anodic mode in various electrolytes to clarify the wear rate and potential stability.

## 7. Conclusions

1. The anodic behavior of the VNZh90 superalloy in a 6 % (wt.) HCl solution in a saturated NaCl solution has been studied. The anodic polarization curve has a shape typical for passivated metals. Strong passivation of the alloy is shown: upon the repeated recording of the anodic curve, the current density of the passivation plateau (indicating the dissolution rate of the alloy) has decreased 2.8 times and is 37 mA/dm$^2$. Thus, the prospects of using the VNZh90 superalloy as a universal cathode-anode material of a reverse electrodialyzer have been shown.

2. The Ni-W alloy has been electroplated. The formation of Ni-W alloy has been confirmed by X-ray diffraction analysis. The anodic behavior of this alloy in a 6 % (wt.) HCl solution in a saturated NaCl solution has been studied. The anodic polarization curve also has a shape typical for passivated metals. On the anodic polarization curve of the alloy with a fresh surface, two dissolution peaks and a clearly pronounced passivation plateau have been revealed. A well-grounded hypothesis has been put forward about the uneven distribution of W in the surface layer of the alloy: the first peak corresponds to a more active phase with a low W content. The hypothesis has been confirmed by the fact that on the repeated anodic curve, the first peak is absent due to the dissolution of the active phase, and the passivation plateaus of the primary and repeated curves coincide. A significant passivity of the alloy has been shown: the passivation current density is 209 mA/dm$^2$. These data have also indicated the possibility and prospects of using the electroplated Ni-W alloy as a universal cathode-anode material of a reverse electrodialyzer. It is recommended to apply a coating on the surface of highly passivated metals (Ti, Mo), and to optimize the composition and deposition method of the alloy, as well as reduce the wear rate.

References


1. Brauns, E. (2008). Towards a worldwide sustainable and simultaneous large-scale production of renewable energy and potable water through salinity gradient power by combining reversed electrodialysis and solar power? Desalination, 219 (1-3), 312–323. doi: https://doi.org/10.1016/j.desal.2007.04.056
2. Doornbusch, G., van der Wal, M., Tedesco, M., Post, J., Nijmeijer, K., Borneman, Z. (2021). Multistage electrodialysis for desalination of natural seawater. Desalination, 505, 114973. doi: https://doi.org/10.1016/j.desal.2021.114973
3. Jang, J. (2021). Ion Exchange Membrane for Reverse Electrodialysis. Academic Journal of Polymer Science, 5 (1). doi: https://doi.org/10.19080/ajop.2021.05.555654
4. Hulme, A. M., Davey, C. J., Tyrrel, S., Pidou, M., McAdam, E. J. (2021). Transitioning from electrodialysis to reverse electrodialysis stack design for energy generation from high concentration salinity gradients. Energy Conversion and Management, 244, 114493. doi: https://doi.org/10.1016/j.enconman.2021.114493
5. Loza, S. A., Smyshlyaev, N. A., Korzhov, A. N., Romanyuk, N. A. (2021). Electrodialysis concentration of sulfuric acid. Chimica Techno Acta, 8 (1), 20218106. doi: https://doi.org/10.15826/chimtech.2021.8.1.06

6. Scialdone, O., D'Angelo, A., Galia, A. (2015). Energy generation and abatement of Acid Orange 7 in reverse electrodialysis cells using salinity gradients. Journal of Electroanalytical Chemistry, 738, 61–68. doi: https://doi.org/10.1016/j.jelechem.2014.11.024
7. Luo, F., Wang, Y., Sha, M., Wei, Y. (2019). Correlations of Ion Composition and Power Efficiency in a Reverse Electrodialysis Heat Engine. International Journal of Molecular Sciences, 20 (23), 5860. doi: https://doi.org/10.3390/ijms20235860
8. Logan, B. E., Elimelech, M. (2012). Membrane-based processes for sustainable power generation using water. Nature, 488 (7411), 313–319. doi: https://doi.org/10.1038/nature11477
9. Luo, X., Cao, X., Mo, Y., Xiao, K., Zhang, X., Liang, P., Huang, X. (2012). Power generation by coupling reverse electrodialysis and ammonium bicarbonate: Implication for recovery of waste heat. Electrochemistry Communications, 19, 25–28. doi: https://doi.org/10.1016/j.elecom.2012.03.004
10. Cusick, R. D., Kim, Y., Logan, B. E. (2012). Energy Capture from Thermolytic Solutions in Microbial Reverse-Electrodialysis Cells. Science, 335 (6075), 1474–1477. doi: https://doi.org/10.1126/science.1219330
11. Altıok, E., Kaya, T. Z., Güler, E., Kabay, N., Bryjak, M. (2021). Performance of Reverse Electrodialysis System for Salinity Gradient Energy Generation by Using a Commercial Ion Exchange Membrane Pair with Homogeneous Bulk Structure. Water, 13 (6), 814. doi: https://doi.org/10.3390/w13060814
12. Ortiz-Imedio, R., Gomez-Coma, L., Fallanza, M., Ortiz, A., Ibañez, R., Ortiz, I. (2019). Comparative performance of Salinity Gradient Power-Reverse Electrodialysis under different operating conditions. Desalination, 457, 8–21. doi: https://doi.org/10.1016/j.desal.2019.01.005
13. Veerman, J., Saakes, M., Metz, S. J., Harmsen, G. J. (2009). Reverse electrodialysis: Performance of a stack with 50 cells on the mixing of sea and river water. Journal of Membrane Science, 327 (1-2), 136–144. doi: https://doi.org/10.1016/j.memsci.2008.11.015
14. Tedesco, M., Brauns, E., Cipollina, A., Micale, G., Modica, P., Russo, G., Helsen, J. (2015). Reverse electrodialysis with saline waters and concentrated brines: A laboratory investigation towards technology scale-up. Journal of Membrane Science, 492, 9–20. doi: https://doi.org/10.1016/j.memsci.2015.05.020
15. Daniilidis, A., Vermaas, D. A., Herber, R., Nijmeijer, K. (2014). Experimentally obtainable energy from mixing river water, seawater or brines with reverse electrodialysis. Renewable Energy, 64, 123–131. doi: https://doi.org/10.1016/j.renene.2013.11.001
16. Othman, N. H., Kabay, N., Guler, E. (2021). Principles of reverse electrodialysis and development of integrated-based system for power generation and water treatment: a review. Reviews in Chemical Engineering. doi: https://doi.org/10.1515/revce-2020-0070
17. Mehdizadeh, S., Kakihana, Y., Abo, T., Yuan, Q., Higa, M. (2021). Power Generation Performance of a Pilot-Scale Reverse Electrodialysis Using Monovalent Selective Ion-Exchange Membranes. Membranes, 11 (1), 27. doi: https://doi.org/10.3390/membranes11010027
18. Vermaas, D. A., Veerman, J., Saakes, M., Nijmeijer, K. (2014). Influence of multivalent ions on renewable energy generation in reverse electrodialysis. Energy & Environmental Science, 7 (4), 1434–1445. doi: https://doi.org/10.1039/c3ee43501f
19. Post, J. W., Goeting, C. H., Valk, J., Goinga, S., Veerman, J., Hamelers, H. V. M., Hack, P. J. F. M. (2010). Towards implementation of reverse electrodialysis for power generation from salinity gradients. Desalination and Water Treatment, 16 (1-3), 182–193. doi: https://doi.org/10.5004/dwt.2010.1093
20. Veerman, J., Saakes, M., Metz, S. J., Harmsen, G. J. (2010). Electrical Power from Sea and River Water by Reverse Electrodialysis: A First Step from the Laboratory to a Real Power Plant. Environmental Science & Technology, 44 (23), 9207–9212. doi: https://doi.org/10.1021/es1009345
21. Spoor, P. B. (2002). Removal of nickel ions from galvanic wastewater streams using a hybrid ion exchange - electrodialysis system. Technische Universiteit Eindhoven. doi: https://doi.org/10.6100/IR551266
22. Deabate, S., Fourgeot, F., Henn, F. (2000). X-ray diffraction and micro-Raman spectroscopy analysis of new nickel hydroxide obtained by electrodialysis. Journal of Power Sources, 87 (1-2), 125–136. doi: https://doi.org/10.1016/s0378-7753(99)00437-1
23. Deabate, S., Fourgeot, F., Henn, F. (1999). Structural and electrochemical characterization of nickel hydroxide obtained by the new synthesis route of electrodialysis. a comparison with spherical β-$Ni(OH)_2$. Ionics, 5 (5-6), 371–384. doi: https://doi.org/10.1007/bf02376001
24. Kovalenko, V., Kotok, V. (2017). Definition of effectiveness of β-$Ni(OH)_2$ application in the alkaline secondary cells and hybrid supercapacitors. Eastern-European Journal of Enterprise Technologies, 5 (6 (89)), 17–22. doi: https://doi.org/10.15587/1729-4061.2017.110390
25. Kovalenko, V. L., Kotok, V. A., Sykchin, A., Ananchenko, B. A., Chernyad'ev, A. V., Burkov, A. A. et. al. (2020). $Al^{3+}$ Additive in the Nickel Hydroxide Obtained by High-Temperature Two-Step Synthesis: Activator or Poisoner for Chemical Power Source Application? Journal of The Electrochemical Society, 167 (10), 100530. doi: https://doi.org/10.1149/1945-7111/ab9a2a
26. Kovalenko, V., Kotok, V. (2018). Synthesis of $Ni(OH)_2$ by template homogeneous precipitation for application in the binder-free electrode of supercapacitor. Eastern-European Journal of Enterprise Technologies, 4 (12 (94)), 29–35. doi: https://doi.org/10.15587/1729-4061.2018.140899
27. Kovalenko, V., Kotok, V. (2017). Study of the influence of the template concentration under homogeneous precepitation on the properties of $Ni(OH)_2$ for supercapacitors. Eastern-European Journal of Enterprise Technologies, 4 (6 (88)), 17–22. doi: https://doi.org/10.15587/1729-4061.2017.106813
28. Kotok, V., Kovalenko, V. (2018). Definition of the aging process parameters for nickel hydroxide in the alkaline medium. Eastern-European Journal of Enterprise Technologies, 2 (12 (92)), 54–60. doi: https://doi.org/10.15587/1729-4061.2018.127764

29. Solovov, V. A., Nikolenko, N. V., Kovalenko, V. L., Kotok, V. A., Burkov, A. A., Kondrat'ev, D. A. et. al. (2018). Synthesis of Ni(II)-Ti(IV) Layered Double Hydroxides Using Coprecipitation At High Supersaturation Method. ARPN Journal of Engineering and Applied Sciences, 13 (24), 9652–9656. Available at: http://www.arpnjournals.org/jeas/research_papers/rp_2018/jeas_1218_7500.pdf
30. Kotok, V., Kovalenko, V., Vlasov, S. (2018). Investigation of NiAl hydroxide with silver addition as an active substance of alkaline batter-ies. Eastern-European Journal of Enterprise Technologies, 3 (6 (93)), 6–11. doi: https://doi.org/10.15587/1729-4061.2018.133465
31. Kovalenko, V., Kotok, V. (2019). Investigation of characteristics of double Ni–Co and ternary Ni–Co–Al layered hydroxides for supercapacitor application. Eastern-European Journal of Enterprise Technologies, 2 (6 (98)), 58–66. doi: https://doi.org/10.15587/1729-4061.2019.164792
32. Kovalenko, V., Kotok, V. (2018). Comparative investigation of electrochemically synthesized (α+β) layered nickel hydroxide with mixture of α-$Ni(OH)_2$ and β-$Ni(OH)_2$. Eastern-European Journal of Enterprise Technologies, 2 (6 (92)), 16–22. doi: https://doi.org/10.15587/1729-4061.2018.125886
33. Kovalenko, V., Kotok, V. (2019). Influence of the carbonate ion on characteristics of electrochemically synthesized layered (α+β) nickel hydroxide. Eastern-European Journal of Enterprise Technologies, 1 (6 (97)), 40–46. doi: https://doi.org/10.15587/1729-4061.2019.155738
34. Kovalenko, V., Kotok, V. (2018). Influence of ultrasound and template on the properties of nickel hydroxide as an active substance of supercapacitors. Eastern-European Journal of Enterprise Technologies, 3 (12 (93)), 32–39. doi: https://doi.org/10.15587/1729-4061.2018.133548
35. Kovalenko, V., Kotok, V. (2020). Bifuctional indigocarminintercalated NiAl layered double hydroxide: investigation of characteristics for pigment and supercapacitor application. Eastern-European Journal of Enterprise Technologies, 2 (12 (104)), 30–39. doi: https://doi.org/10.15587/1729-4061.2020.201282
36. Kovalenko, V., Kotok, V. (2020). Tartrazine-intercalated Zn–Al layered double hydroxide as a pigment for gel nail polish: synthesis and characterisation. Eastern-European Journal of Enterprise Technologies, 3 (12 (105)), 29–37. doi: https://doi.org/10.15587/1729-4061.2020.205607
37. Kovalenko, V., Kotok, V. (2020). Determination of the applicability of ZnAl layered double hydroxide, intercalated by food dye Orange Yellow S, as a cosmetic pigment. Eastern-European Journal of Enterprise Technologies, 5 (12 (107)), 81–89. doi: https://doi.org/10.15587/1729-4061.2020.214847
38. Vermaas, D. A., Kunteng, D., Veerman, J., Saakes, M., Nijmeijer, K. (2014). Periodic Feedwater Reversal and Air Sparging As Antifouling Strategies in Reverse Electrodialysis. Environmental Science & Technology, 48 (5), 3065–3073. doi: https://doi.org/10.1021/es4045456
39. Tedesco, M., Scalici, C., Vaccari, D., Cipollina, A., Tamburini, A., Micale, G. (2016). Performance of the first reverse electrodialysis pilot plant for power production from saline waters and concentrated brines. Journal of Membrane Science, 500, 33–45. doi: https://doi.org/10.1016/j.memsci.2015.10.057
40. Kim, H.-K., Lee, M.-S., Lee, S.-Y., Choi, Y.-W., Jeong, N.-J., Kim, C.-S. (2015). High power density of reverse electrodialysis with pore-filling ion exchange membranes and a high-open-area spacer. Journal of Materials Chemistry A, 3 (31), 16302–16306. doi: https://doi.org/10.1039/c5ta03571f
41. Burmistr, M. V., Boiko, V. S., Lipko, E. O., Gerasimenko, K. O., Gomza, Y. P., Vesnin, R. L. et. al. (2014). Antifriction and Construction Materials Based on Modified Phenol-Formaldehyde Resins Reinforced with Mineral and Synthetic Fibrous Fillers. Mechanics of Composite Materials, 50 (2), 213–222. doi: https://doi.org/10.1007/s11029-014-9408-0
42. Vlasova, E., Kovalenko, V., Kotok, V., Vlasov, S., Sukhyy, K. (2017). A study of the influence of additives on the process of formation and corrosive properties of tripolyphosphate coatings on steel. Eastern-European Journal of Enterprise Technologies, 5 (12 (89)), 45–51. doi: https://doi.org/10.15587/1729-4061.2017.111977
43. Gaona-Tiburcio, C., Aguilar, L. M. R., Zambrano, R. P., Estupiñán, L. F., Cabral, M. J. A., Nieves-Mendoza, D. et. al. (2014). Electrochemical Noise Analysis of Nickel Based Superalloys in Acid Solutions. International Journal of Electrochemical Science, 9 (2), 523–533.
44. Ciesla, M., Manka, M., Gradon, P., Binczyk, F. (2014). Impact of a Structure on Durability of Modified Nickel-Base Superalloys in Creep Conditions. Archives of Metallurgy and Materials, 59 (4), 1559–1563. doi: https://doi.org/10.2478/amm-2014-0264
45. Kovalenko, V., Kotok, V. (2017). Selective anodic treatment of W(WC)-based superalloy scrap. Eastern-European Journal of Enterprise Technologies, 1 (5 (85)), 53–58. doi: https://doi.org/10.15587/1729-4061.2017.91205
46. Kovalenko, V., Kotok, V. (2020). Investigation of the anodic behavior of w-based superalloy for electrochemical selective treatment. Eastern-European Journal of Enterprise Technologies, 6 (12 (108)), 55–60. doi: https://doi.org/10.15587/1729-4061.2020.218355
47. Kovalenko, V., Kotok, V., Vlasov, S. (2018). Development of the electrochemical synthesis method of ultrafine cobalt powder for a superalloy production. Eastern-European Journal of Enterprise Technologies, 2 (6 (92)), 41–47. doi: https://doi.org/10.15587/1729-4061.2018.126928
48. Kovalenko, V., Kotok, V., Vlasov, S. (2018). Definition of synthesis parameters of ultrafine nickel powder by direct electrolysis for application in superalloy production. Eastern-European Journal of Enterprise Technologies, 1 (6 (91)), 27–33. doi: https://doi.org/10.15587/1729-4061.2018.121595
49. Kuznetsova, O. G., Levin, A. M., Sevostyanov, M. A., Bolshih, A. O. (2019). Electrochemical recycling of nickel-cobalt-containing tungsten alloys. IOP Conference Series: Materials Science and Engineering, 525, 012088. doi: https://doi.org/10.1088/1757-899x/525/1/012088

50. Kuznetsova, O. G., Levin, A. M., Sevast'yanov, M. A., Tsybin, O. I., Bol'shikh, A. O. (2019). Electrochemical Oxidation of a Heavy Tungsten-Containing VNZh-Type Alloy and Its Components in Ammonia–Alkali Electrolytes. Russian Metallurgy (Metally), 2019 (5), 507–510. doi: https://doi.org/10.1134/s0036029519050057
51. Kuznetsova, O. G., Levin, A. M., Sevostyanov, M. A., Tsybin, O. I., Bolshikh, A. O. (2020). Changes in electrochemical properties of a heavy tungsten alloy during its processing under the influence of DC current in ammonia-alkali solutions. IOP Conference Series: Materials Science and Engineering, 848, 012045. doi: https://doi.org/10.1088/1757-899x/848/1/012045
52. Kuznetsova, O. G., Levin, A. M., Sevostyanov, M. A., Tsybin, O. I., Bolshikh, A. O. (2020). AC electrochemical oxidation of nickel and VNZh alloy in alkaline-ammonium solutions. IOP Conference Series: Materials Science and Engineering, 848, 012046. doi: https://doi.org/10.1088/1757-899x/848/1/012046
53. Sridhar, T. M., Eliaz, N., Gileadi, E. (2005). Electroplating of Ni4W. Electrochemical and Solid-State Letters, 8 (3), C58. doi: https://doi.org/10.1149/1.1857114
54. Eliaz, N., Sridhar, T. M., Gileadi, E. (2005). Synthesis and characterization of nickel tungsten alloys by electrodeposition. Electrochimica Acta, 50 (14), 2893–2904. doi: https://doi.org/10.1016/j.electacta.2004.11.038
55. Zhu, L., Younes, O., Ashkenasy, N., Shacham-Diamand, Y., Gileadi, E. (2002). STM/AFM studies of the evolution of morphology of electroplated Ni/W alloys. Applied Surface Science, 200 (1-4), 1–14. doi: https://doi.org/10.1016/s0169-4332(02)00894-2
56. Trelewicz, J. R., Schuh, C. A. (2009). Hot nanoindentation of nanocrystalline Ni–W alloys. Scripta Materialia, 61 (11), 1056–1059. doi: https://doi.org/10.1016/j.scriptamat.2009.08.026
57. Sulitanu, N., Brinza, F. (2003). Structure-properties Relationships in Electrodeposited Ni-W Thin Films with Columnar Nanocrystallites. Journal of Optoelectronics and Advanced Materials, 5 (2), 421–427.
58. Schloßmacher, P., Yamasaki, T. (2000). Structural Analysis of Electroplated Amorphous-Nanocrystalline Ni-W. Microchimica Acta, 132 (2-4), 309–313. doi: https://doi.org/10.1007/s006040050074
59. Cesiulis, H., Podlaha-Murphy, E. J. (2003). Electrolyte Considerations of Electrodeposited Ni-W Alloys for Microdevice Fabrication. Materials Science (Medžiagotyra), 9 (4), 329–333. Available at: https://matsc.ktu.lt/index.php/MatSc/article/view/26731
60. Yamasaki, T. (2000). High-strength Nanocrystalline Ni-W Alloys Produced by Electrodeposition. Mater. Phys. Mech., 1, 127–132. Available at: https://www.ipme.ru/e-journals/MPM/no_2100/yamasaki/yamasaki.pdf
61. Esther, P., Joseph Kennady, C., Saravanan, P., Venkataehalam, T. (2009). Structural and Magnetic Properties of Electrodeposited Ni-Fe-W Thin Films. Journal of Non-Oxide Glasses, 1 (3), 301–309. Available at: https://chalcogen.ro/301_Esther.pdf
62. Nenastina, T., Bairachnaya, T., Ved, M., Shtefan, V., Sakhnenko, N. (2007). Electrochemical Synthesis of Catalytic Active Alloys. Functional Materials, 14 (3), 395–400. Available at: http://dspace.nbuv.gov.ua/bitstream/handle/123456789/136993/24-Nenastina.pdf?sequence=1
63. Zemanová, M., Krivosudská, M., Chovancová, M., Jorík, V. (2011). Pulse current electrodeposition and corrosion properties of Ni–W alloy coatings. Journal of Applied Electrochemistry, 41 (9), 1077–1085. doi: https://doi.org/10.1007/s10800-011-0331-y
64. Alimadadi, H., Ahmadi, M., Aliofkhazraei, M., Younesi, S. R. (2009). Corrosion properties of electrodeposited nanocrystalline and amorphous patterned Ni–W alloy. Materials & Design, 30 (4), 1356–1361. doi: https://doi.org/10.1016/j.matdes.2008.06.036